

Impregnated Paper-Based Decorative Laminates Prepared from Lignin-Substituted Phenolic Resins

Marion Thébault¹, Ya Li¹, Christopher Beuc¹, Stephan Frömel-Frybort^{1,2}, Edith-Martha Zikulnig-Rusch¹, Larysa Kutuzova³ and Andreas Kandelbauer^{3,*}

¹Kompetenzzentrum Holz (Wood K Plus), Altenberger Straße 69, A-4040, Linz, Austria

²University of Life Sciences and Natural Resources (BOKU), Universitäts- und Forschungszentrum Tulln (UFT), Tulln, A-3430, Austria

³Reutlingen University, Lehr- und Forschungszentrum Process Analysis & Technology (PA&T), School of Applied Chemistry, Reutlingen, D-72762, Germany

*Corresponding Author: Andreas Kandelbauer. Email: andreas.kandelbauer@reutlingen-university.de

Received: 03 February 2020; Accepted: 13 July 2020

Abstract: High Pressure Laminates (HPL) panels consist of stacks of self-gluing paper sheets soaked with phenol-formaldehyde (PF) resins. An important requirement for such PFs is that they must rapidly penetrate and saturate the paper pores. Partially substituting phenol with bio-based phenolic chemicals like lignin changes the physico-chemical properties of the resin and affects its ability to penetrate the paper. In this study, PF formulations containing different proportions of lignosulfonate and kraft lignin were used to prepare paper-based laminates. The penetration of a Kraft paper sheet was characterized by a recently introduced, new device measuring the conductivity between both sides of the paper sheet after a drop of resin was placed on the surface and allowed to penetrate the sheet. The main target value measured was the time required for a specific resin to completely penetrate the defined paper sample (“penetration time”). This penetration time generally depends on the molecular weight distribution, the flow behavior and the polarity of the resin which in turn are dependent on the manufacturing conditions of the resin. In the present study, the influences of the three process factors: (1) type of lignin material used for substitution, (2) lignin modification by phenolation and (3) degree of phenol substitution on the penetration times of various lignin-phenolic hybrid impregnation resins were studied using a complete two-level three-factorial experimental design. Thin laminates made with the resins diluted in methanol were mechanically tested in terms of tensile and flexural strains, and their cross-sections were studied by light microscopy.

Keywords: Lignin; phenol-formaldehyde resin (PF); decorative laminate; impregnated paper

1 Introduction

Paper-based laminates with PF-impregnated core layers are extensively applied in interior spaces for wet-room applications like bathroom furniture (e.g., high-quality furniture elements with integrated sinks)



This work is licensed under a Creative Commons Attribution 4.0 International License, which permits unrestricted use, distribution, and reproduction in any medium, provided the original work is properly cited.

and exterior applications (e.g., as especially durable and long-lasting decorative laminate panels for exterior wall claddings). The bulk laminate consists of Kraft paper sheets having a raw weight of 80–260 g/m². The Kraft papers are soaked with PF oligomers and pre-dried at elevated temperature to yield self-gluing impregnated papers, which are subsequently assembled to stacks of 10–40 sheets. Since PF impregnated papers are always black, freedom in design and individual visual appearance of the decorative laminate is accomplished by melamine formaldehyde (MF) resin impregnated decorative papers as surface sheets [1]. The PF core is laminated together with the MF surface sheets in a hot press to give the final, so-called “high-pressure laminate” (HPL) [2]. The PF resins used in the laminates industry are mainly water borne, liquid resols of low molecular weight with good penetration properties [3]. Resols are PF resins prepared under alkaline conditions with sodium hydroxide as the catalyst [4].

For environmental as well as economic reasons, the substitution of the fossil resources-based phenol monomer by a suitable renewable raw material is of high interest. Recently, a number of innovative bio-based composite materials have been described [5–7] and a wide variety of renewable resources have been applied to substitute or replace fossil-based raw materials for thermosets and binders. Sucrose, for instance, has been employed as a binder for plywood [8–11]. It was also successfully applied as a supplement to partially replace melamine in melamine-formaldehyde-based decorative laminates [12]. Citric acid-based binders have been developed for gluing wood-moldings [13] and combinations of citric acid with sucrose produced eco-friendly binder materials for plywood [14,15]. Many plant-protein-based green composites have been described in the recent literature [16]. For instance, plant protein-based binders derived from soy bean have been developed for gluing plywood [17] and soy protein isolate (ISO) has been used even for the development of self-healable and antibacterial soy protein-based films of high mechanical strength [18] or for the functionalization of boron-nitride nanosheets [19]. Thermosets from chemically modified plant-oils have also frequently been exploited as binders and coatings [20–26]. Various types of self-gluing boards utilizing the native binder material inherent to lignocellulosic materials have also been developed [27]. They are mainly building upon the lignin present in the raw material which acts as natural phenol resin glue. Examples for this include self-binding wood fiberboards [28,29] or binder-less reed-like plant derived composites [30,31]. Tannin-based raw materials also play a major role in the development of bio-based composites [32–34].

Among these bio-based materials, lignin as the most abundant natural polyphenolic polymer plays a major role as a green binder material [35–37] and potential substitute for phenolic or similar compounds [38,39]. The complete or partial replacement of phenol by lignin or other renewable phenolic compounds was the topic of a recent review [40].

Many different phenolic resins containing various types of lignin were assessed for their gluing performance as binder materials of engineered wood [41–44] or for their suitability as impregnation resins for the manufacture of decorative laminates [40,44–47]. With the latter application, the homogenous impregnation and deep saturation of Kraft papers is very important. Inhomogeneous impregnation and saturation will lead to laminate defects such as blisters, warping, or delamination [48,49]. The substitution of phenol by lignin causes significant changes in resin properties [50]. Co-condensing lignin with phenol and formaldehyde will lead to altered interaction between resin and the porous paper matrix compared to pure PF resin. The important effects of both resin and paper on the impregnation process were summarized recently in a review [51]. It is problematic to discern and quantitatively model rate and degree of penetration. Difficulties in predicting imbibition performance in a system resin/absorbing paper often arise, for instance, from insufficient accuracy in measuring contact angles and surface tensions of both materials and from the complexity in characterizing the 3D porous geometry of the substrate. A relatively simple and rapid method to characterize imbibition behavior of a liquid into a porous substrate was introduced earlier [52]. This method is based on measuring the conductivity induced by the liquid flowing through the porous substrate and was used to characterize the impregnation behavior of neat phenol-formaldehyde resin

formulations [53]. Besides resin viscosity, number average molecular weight and surface tension were found to have a great influence on paper penetration. Substitution of part of the phenol by lignin significantly changes these properties [54] and thus, impregnation performance.

Much experimental evidence has been described regarding lignin-containing phenolic resins. However, in most studies available in the scientific literature, emphasis has been given on the adhesive properties mainly for gluing and bonding applications, i.e., on binder resins. Impregnation resins despite their commercial importance are heavily underrepresented. The present study is intended to fill this gap to some extent and provide experimental data specifically of interest for the application of such resins in impregnation processes. The detailed effects of specific process parameters have not yet been studied in a systematic manner to identify the quantitative influences of relevant factors. In the present study, a statistical experimental design is used (a) to identify the statistical significance of three selected and presumably relevant factors, (b) to quantify the effects of these factors, (c) and to identify whether there are synergistic actions between these factors (so-called “two-factor interaction (2FIA) effects”) on a specific response. The method of choice for this is to apply a full factorial experimental design. Factorial experiments are orthogonal experimental designs that allow mathematical isolation of the effects that some controlled variables exhibit on a response. An arbitrary number of responses can be studied with the same set of process factor variations. In a two-level factorial experiment, the factor levels of the investigated control variables are simultaneously varied on two settings in a systematic way as to determine each factor effect independent from all other factors studied. For this, a number of 2^n experiments is performed, n being the number of factors studied. This distinguishes this approach from the one-factor-at-a-time (OFAT) experimental set-ups that are usually found in the scientific literature. In such OFATs, no systematic and simultaneous factor level variations are employed. Instead, the influence of each factor is studied separately in a sequence of experiments while the levels of all other factors are kept constant. Such an experimental design cannot identify 2FIAs at any circumstances which is the major limitation of this traditional approach besides being very ineffective and time-consuming among other disadvantages. Being able to identify potential synergies is of great importance since with many technical processes, synergistic actions often have a greater impact on the system than the single factors for themselves.

In the present study, the impregnation properties of lignin-modified phenolic resins with a special kind of Kraft paper (the so called “saturating” Kraft paper) are investigated. The penetration behavior of nine different partially lignin-substituted phenol formaldehyde resins into Kraft paper is described. Impregnated papers were characterized by Inverse Gas Chromatography (IGC) to measure the different specific surface areas, for each resin system. Finally, thin laminates were prepared from the impregnated paper sheets and tested for their mechanical properties.

2 Materials and Methods

2.1 Chemicals

Phenol (99% purity), formaldehyde (aqueous solution with a formaldehyde content of 37%) and sulfuric acid (96% aqueous solution) were supplied from Roth Chemicals (Karlsruhe, Germany). Sodium hydroxide was purchased from Sigma Aldrich (Saint-Louis, Missouri, United States). Sodium lignosulfonates DP 400 was purchased from Westvaco Corp. (Charleston, South Carolina, United States), and alkali lignin (Kraft) from Sigma Aldrich (Steinheim, Germany).

2.2 Resin Preparation

Phenol and lignin-phenol resins were prepared following the general procedure described in [50]. All resins were synthesized in a three-necked round bottom flask. After adjusting the pH to 8 with diluted NaOH, the reaction mixture containing the reagents in amounts according to the experimental design was

heated to 90°C and kept at this temperature for two hours. In some resins, phenol was substituted by lignosulfonate or Kraft lignin to a percentage of 30% or 50%. Lignin was either used as such or subjected to phenolation modification prior to the preparation of the lignin phenol hybrid resins. Phenolation was carried out with sulfuric acid (72%) at 100°C for three hours.

The experimental design was a two-level three-factorial screening experiment. The three factors analyzed were: (1) lignin type (either sodium lignosulfonate or Kraft lignin), (2) lignin modification type (either with or without phenolation modification), and (3) degree of phenol substitution by lignin (either 30% or 50% of the mass of phenol required for a P:F molar ratio of 1:1,8). The factor level settings for the resins are summarized in [Tab. 1](#). Resin synthesis and their properties (molecular weight distribution, infrared absorbance, thermal properties as well as rheological behavior) are described in further detail elsewhere [50].

Table 1: Experimental settings used to prepare the various lignin-phenolic hybrid model resins synthesized with different types of lignin materials, treatments, and substitution levels

Resin	Lignin material	Previous treatment before synthesis	Substitution level (w/w Phenol)
PF	–	–	0%
L30PF	Lignosulfonates	–	30%
LP30PF	Lignosulfonates	Phenolation	30%
L50PF	Lignosulfonates	–	50%
LP50PF	Lignosulfonates	Phenolation	50%
K30PF	Kraft lignin	–	30%
KP30PF	Kraft lignin	Phenolation	30%
K50PF	Kraft lignin	–	50%
KP50PF	Kraft lignin	Phenolation	50%

2.3 Resin Properties

Surface tension was determined using a DCAT11EC device (DataPhysics Instruments GmbH, Filderstadt, Germany) upon dilution with MeOH to a solid content of 45%. Measurements were always performed at 25°C. Contact angles were determined applying the sessile drop method. The device used was an OCA 35 (DataPhysics Instruments GmbH, Filderstadt, Germany). Dynamic viscosities were measured with a Physica MCR 101 rheometer (Anton Paar GmbH, Graz, Austria). All measurement protocols are given in more detail in [50].

2.4 Raw Paper

Kraft paper sheets Durasorb Saturating Kraft with a paper weight of 250.0 g/m², Caliper 386, and a size core of 76 mils were provided from Kapstone Paper and Packaging Corp. (Northbrook, Illinois, United States). The wet strength was 340 ± 20 N/m in cross direction and 566.7 ± 40 N/m in machine direction. The Gurley air permeation was 9 ± 0.6 s.

2.5 Penetration Time Measurements

A penetration measurement device recently patented [52] was used to characterize the penetration behavior of the lignin-modified PF resins with Kraft paper.

The measurement principle is based on changes in conductivity between the top and bottom sides of the penetrated substrate [52] and briefly summarized in Fig. 1. Penetration time was measured for all resins after placing a drop of the resin on the upper surface. Once a resin drop is deposited between E1 and E2, the changes in conductivity upon resin flow through the paper substrate are measured between the upper electrodes, E1 and E2, and between the upper electrode E1 and the bottom electrode E3. Penetration time was determined as the time required to achieve a steady conductivity signal of 14 mA between E1 and E3. For all resins, the same Kraft paper was used. All penetration measurements were performed 12 times for each resin system.

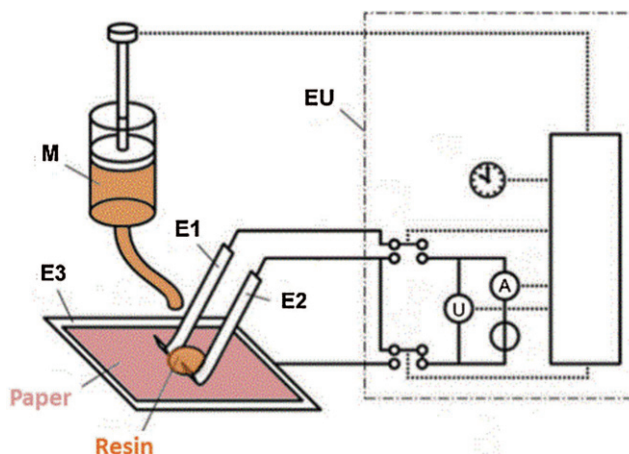


Figure 1: (a) Penetration testing device fitted with a resin pipette and a sample of paper sheet; (b) Schematic of the device; EU: Electronic unit; E1, E2, E3: Top and bottom electrodes; M: syringe containing the tested liquid

2.6 Specific Surface Area of Raw and Impregnated Papers

The specific surface area of raw and impregnated papers was measured via Inverse Gas Chromatography (IGC). The measurements were conducted on an Agilent 6890 gas chromatograph equipped with FID and using the Chemstation Control Software Version 1.5 (Porotec GmbH, Hofheim/Ts., Germany). IGC data were evaluated with the software by Surface Measurement Systems, Alperton Middlesex, London, UK. Impregnated paper samples were cut into small strips (18 cm in length and 3–4 mm in width) and filled in silanized glass columns (inner diameter \varnothing of 4 mm). All samples were conditioned for 4 hours under helium gas flow ($20 \text{ cm}^3 \text{ min}^{-1}$) at 35°C prior to the actual measurement.

The specific surface area (BET-surfaces) of raw and impregnated Kraft paper sheets was determined by injecting n-hexane with 0.10, 0.15, 0.20, 0.25, 0.30, 0.35, 0.40, 0.45, 0.50 p/p_0 at 35°C .

2.7 Preparation of Paper Laminates and Mechanical Properties of Laminates Prepared from Impregnated Papers

All prepared resins were used for impregnating Kraft paper samples. Small pieces of Kraft paper ($30 \times 30 \text{ cm}$) were impregnated manually on a laboratory scale using a bath of resin at ambient temperature. They were dipped into the resin solution for 5 s. Then, excess resin was removed by squeezing the wet impregnated paper between two rollers. For each sheet of impregnated paper, resin uptake was 40–48% relative to the paper weight. The impregnated pieces were mounted on a support with clips and placed in a ventilated oven at 145°C for 2 min to dry and pre-cure the resins. At this stage (B-stage), the resin is viscoelastic and still able to flow if pressure is applied.

Some samples of such pre-pregs were kept for measuring the specific surface area, and little pieces of laminates consisting of a stack of five sheets were prepared in a hot press at 15 bar, a temperature of 150°C, and for a pressing time of 5 minutes. Conventionally, High Pressure Laminates (HPL) are glued at pressures above 50 bar (according to the standard EN 438-4:2005); typical pressure conditions are between 70 and 100 bar. In the present study, we observed that such high values of pressure lead to massive damage of the laminates similar to the effects described in [51]. This damage was probably due to the relatively large moisture content and entrapped air in the hand-impregnated paper sheets. At 15 bar, however, defect-free laminates were obtained.

3 Results and Discussion

3.1 Effect on Penetration Behavior of the Model Resins

Penetration measurements were used to determine the penetration time of the various resins. Some typical results for the penetration time measurements are given in Fig. 2. The average values for penetration time derived from at least twelve repeat measurements for each resin sample are summarized in Fig. 3. The characteristic shape of the conductivity time course obtained from penetration time measurements is depicted in Fig. 2. One sees the changes in conductivity as measured between the electrode pairs E1–E2 and E1–E3 during penetration of the resin through the Kraft paper sheet. Between the top and bottom electrodes (E1–E3), the conductivity takes some seconds or fractions of a second to rise once the drop is deposited. In contrast, the conductivity on the top side (E1–E2) continuously decreases from a maximum value at different rates depending on the resin system applied. This is partially due to the horizontal spreading of the drop on the paper surface and partially due to the vertical absorption across the paper. In some systems, the decrease in conductivity measured between E1 and E2 accelerates (while at the same time a simultaneous rise in conductivity between E1 and E3 takes place) and decelerates later again. The control resin P had the lowest value of E1–E2 conductivity at the beginning of the measurements (below 13 mA) and at the end of drop imbibition (4–8 mA). It had the lowest crossing end time as deduced from the very early rise in conductivity between E1 and E3.

Independent of the lignin type, resins with a substitution level of 50%, display, on average, a higher maximum value of conductivity between E1 and E2 than the resins with only 30% substitution. The liquids tend to remain on the surface of the paper longer when the amount of lignin is higher as seen from the smaller decrease in conductivity.

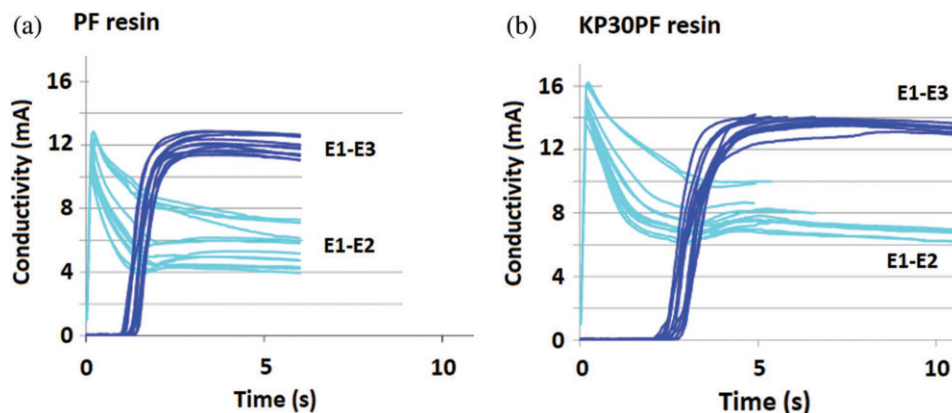


Figure 2: Representative measurements of penetration behavior, shown for the pristine PF reference resin and the lignin-modified resin containing 30% Kraft lignin (KP30PF). Time course of conductivity between the electrodes E1 and E2 at the paper top side of the test paper (E1–E2, light blue lines) and between the top and bottom electrodes E1 and E3 (E1–E3, dark blue lines) after depositing a drop on the surface of a paper testing sheet

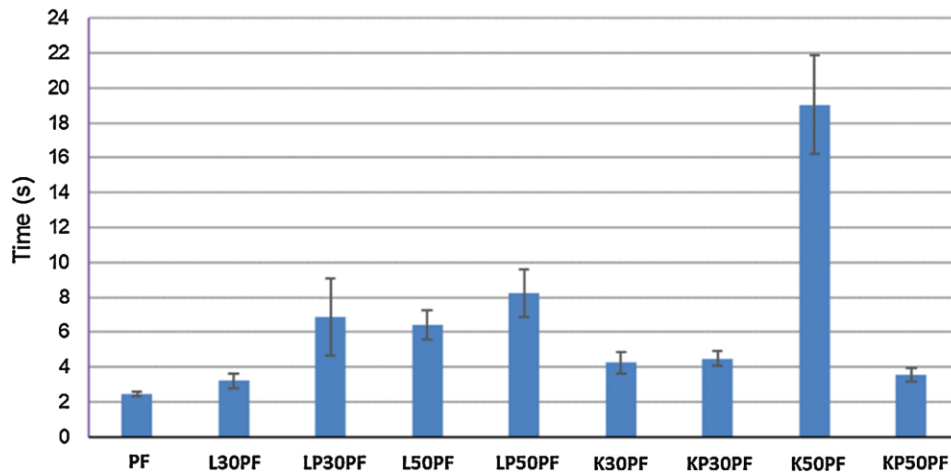


Figure 3: Penetration time all resin systems

Table 2: Resins surface tension characteristics and viscosity behavior (Data from [50])

Resin	Surface tension* (mN/m)	Polar component γ_L^P ** (mN/m)	Dispersive component γ_L^D ** (mN/m)	Viscous profile	Range of viscosity (mPa s)****
PF	32,17	NA***	NA***	Newtonian-Dilatant	14.6–17.7
L30PF	30,83	0.79	30.04	Dilatant	24.4–44.6
LP30PF	32,25	0.96	31.29	Dilatant	20.6–27.1
L50PF	28,71	0.53	28.18	Shear-thinning	190–304
LP50PF	30,88	0.53	30.34	Bingham-Dilatant	41.1–65.3
K30PF	29,69	0.66	29.03	Dilatant	31.6–87.5
KP30PF	33,41	1.45	31.96	Dilatant	30.1–45.9
K50PF	33,55	0.72	32.82	Bingham	94.4–246
KP50PF	33,04	1.29	31.75	Newtonian-Dilatant	23.3–26.5

* With water removal and solid content adjustment around 45% with methanol.

** Calculated from contact angles measurements.

*** Not Analyzed: the contact angle was too low to be detected.

**** Measured at various shear rates between 20 s^{-1} (low value given) and 100 s^{-1} (high value given).

Tab. 2 summarizes some characteristic resin properties.

It was demonstrated earlier [53] that at relatively low viscosities, the penetration time is predominantly dependent on the surface tension of the liquid. However, in the present study, it seems that other parameters play a role as well. The viscosities of the resins PF and LP30PF are rather low and differ only in less than 10 mPa s. Moreover, their surface tension values are very similar. Nevertheless, PF wets glass much more readily than LP30PF. This suggests that the polar component of the surface energy of PF is higher than that of LP30PF. Considering that paper fibers, like glass, have a very polar surface energy component due to the numerous hydroxyl groups present, resins that are more likely to wet the paper and penetrate it rapidly will also be those with a higher polar/dispersive surface energy ratio (**Tab. 2**), e.g., with a smaller contact angle with glass (**Tab. 2**). Thus, as PF is more polar and less viscous than LP30PF, it seems logic that it penetrated the paper more rapidly.

The average end times of imbibition for each resin system are summarized in Fig. 3. The penetration times of the resin droplets for completely penetrating the paper range from 2.5 to 8.2 s for all resins but one which had an especially long penetration time of 19.0 ± 2.8 s (resin K50PF). As shown in Fig. 2, a rise in conductivity between the top and bottom side of paper is detected only 10 to 15 s after a droplet of this resin was placed on the surface, and the conductivity increase is much slower than with the other resins. This could be due to the observed Bingham viscosity behavior (Tab. 2) with this resin: as no shear effect is applied to the droplet once it is deposited on the paper surface, the cohesive forces between the resin molecules hamper its mobility, which might impede penetration in the observed way. The surface tension value, 33.55 mN/m (Tab. 2) was the highest one observed within the set of studied resins. It could have also played a role in the long penetration time of this resin. Resin LP50PF, which also behaves like a Bingham liquid (Tab. 2), had the second longest crossing time through paper. Regarding the time course of the conductivities measured at the top electrodes (Fig. 2), a similar trend was observed that is not encountered with any of the other resins: a slow decrease in conductivity that never falls below 12 mA, even after the liquid had completely penetrated the paper cross-section. This suggests that a relatively large amount of the liquid stays on the top surface during and even after penetration.

Fig. 4 shows photographs of some specimens of the impregnated/imbibed paper samples tested. All resins that contained lignin were initially black-colored liquids before they were used in the impregnation experiments whereas the control resin PF was a yellow liquid. The impregnation patterns produced by the resins containing lignosulfonates mostly show lighter colors on the bottom side (resins LP30PF, L50PF and LP50PF). Some bright, cured resin aggregations are visible on the top side, which means that not all components of the resins were able to penetrate completely through the paper.

The paper sample penetrated by the resin K50PF is the only specimen where a film had formed on the bottom side, outside on the surface of the paper. This implies that part of the resin liquid succeeded in penetrating the paper cross-section completely without being retained at all by the fibers inside of the sheet. Another part, however, remained on the top side. This is also confirmed by a comparatively high value of conductivity observed between E1 and E2. The remainder imbibed to some extent.

3.2 Effect on Paper Saturation of Impregnated Papers

Specific surface area of the raw and impregnated papers was determined with Inverse Gas Chromatography. In this method, an unpolar volatile probe molecule is adsorbed onto the paper surface which is used as the stationary phase. The specific surface area of the impregnated papers or “pre-pregs” is a reasonably good quantitative indicator to judge the level of saturation (filling of the pores) of a paper sheet with the resin (Fig. 5). All specific surface areas decreased upon impregnation significantly from 4.44 ± 0.28 m²/g (raw paper) to 0.7–2 m²/g (impregnated papers).

For lignin-phenolic hybrid resins that contained lignosulfonates, the resulting pre-pregs all showed significantly larger surface areas than those without lignin or where phenol was substituted by Kraft lignin. This suggests that lignosulfonate modified PF resins cannot fill the papers as effectively. The pre-pregs with the resin K50PF also showed comparatively high values of surface area. K50PF displays a Bingham-like viscosity profile, i.e., its viscosity decreases at higher shear rates whereas when low shear forces or none at all are applied, resin flow becomes rather limited. The manual impregnation in the laboratory was performed by simply soaking the paper in a small amount of resin and squeezing it through rolls at low speed. Under these conditions, the K50PF liquid resin remained relatively highly viscous and immobile and was not very likely to readily enter small pores.

Although the factor phenolation was not statistically significant (Tab. 3), the standard deviation in surface area is significantly larger when the lignosulfonates in the resins were phenolated than when they were not. This suggests that the distribution of resin inside the pores of the paper is not homogeneous

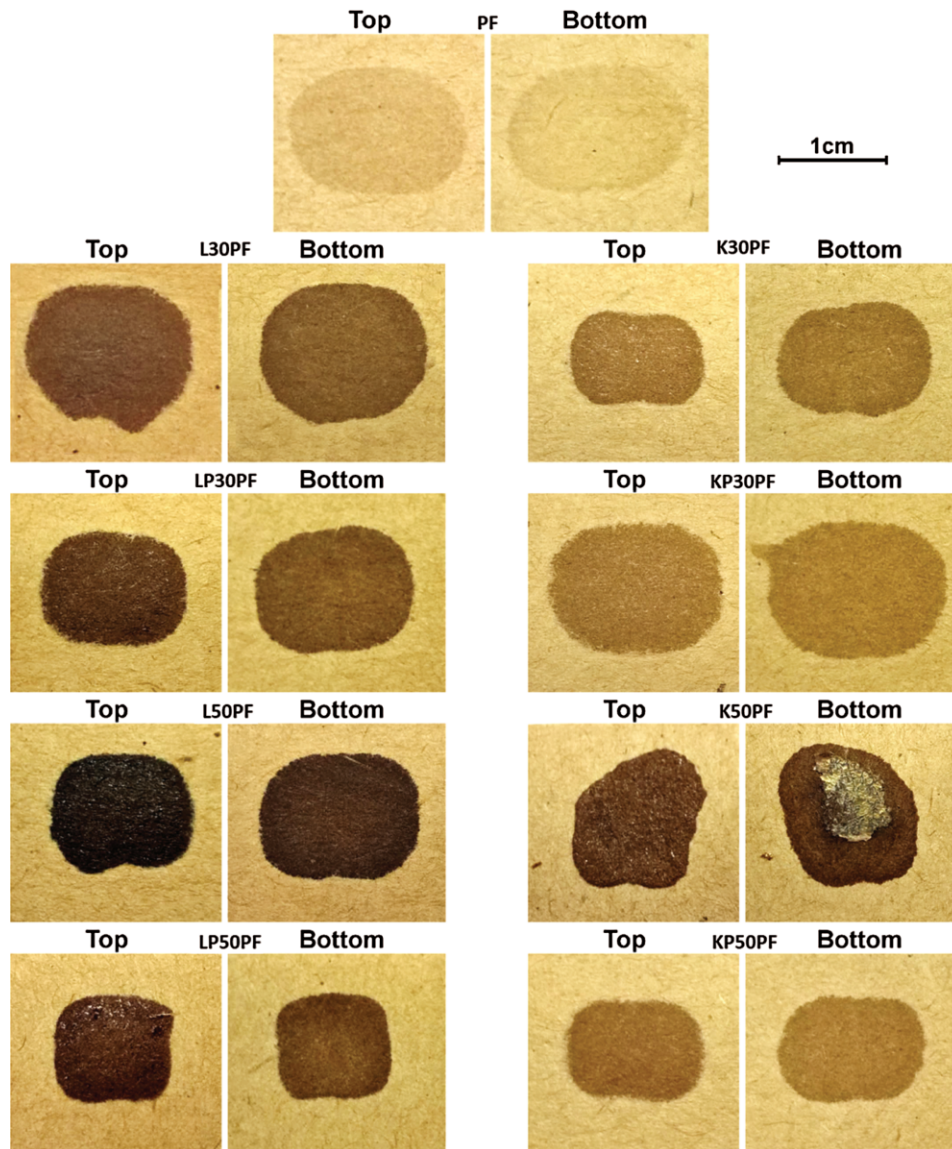


Figure 4: Droplet patterns of resins on kraft papers on the top and bottom sides. The drops were deposited of the top side during the tests

from one pre-preg sample to another. This could be due to a large variety of molecules of different molecular weights present in the resin resulting from the phenolation modification of liginosulfonates. A similar difference in standard deviations was also observed for these resins in penetration times (Fig. 3), which supports this hypothesis. Fig. 6 summarizes the effects of the two statistically significant factors “lignin type” and “degree of substitution.”

3.3 Effect on Mechanical Properties of the Test Laminates

The 5-ply laminates were 1.25 to 1.61 mm thick in average. Their crosscut sections were visually evaluated with a microscope (Fig. 7). Their densities and mechanical properties (tensile and flexural strengths, flexural modulus) are listed in Tab. 4. A few non-impregnated paper fibers in the cores of some laminates are clearly visible. The laminate made from the resin L30PF showed a very inhomogeneous

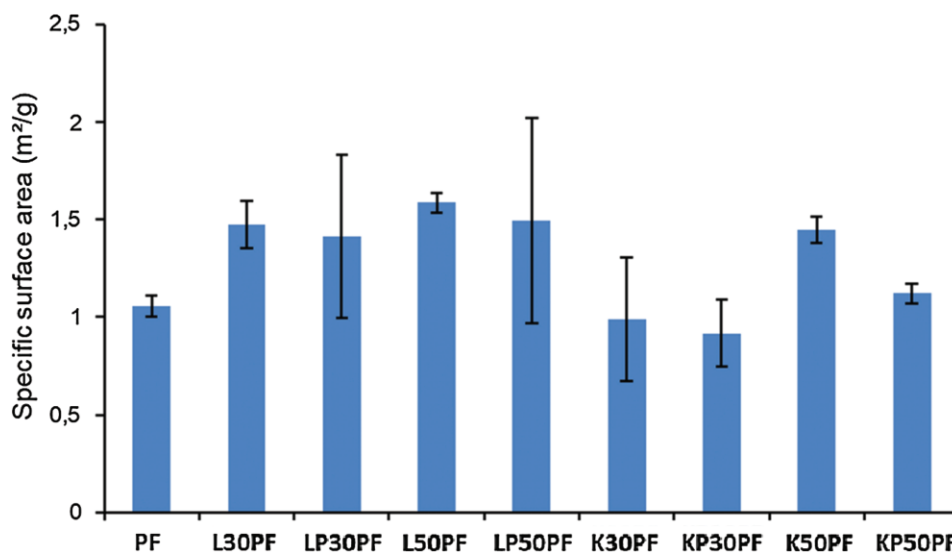


Figure 5: Specific surface areas of the impregnated papers. The specific surface area of pristine Kraft paper is 4.44 ± 0.28 m²/g

Table 3: ANOVA analysis of the effects influencing the response “specific surface area” papers impregnated with the lignin-phenol hybrid resins

	Sum of Squares	<i>F</i> -value	<i>p</i> -value	R ²	R ² _{adjusted}	R ² _{predicted}
Model ^{*)}	0.4129	10.87	0.0216	0.8907	0.8088	0.5629
Effects						
A: Lignin	0.2812	22.21	0.092			0.1875
B: Phenolation	0.0392	3.10	0.1533			-0.0700
C: Substitution	0.0925	7.30	0.0540			0.1075
Residual	0.4635					

resin distribution and delamination defects on one side (Fig. 7b). Its mechanical performance was worst (Tab. 4). According to the EN ISO 1183-1 standard classifying the HPL products, the required density is at least 1.35 or higher. Only the boards made with the resins PF and KP30PF complied with this threshold, and with these laminates, the best overall mechanical properties and resin distribution homogeneity were encountered as well. High values for mechanical properties show also the laminates impregnated with the resin KP50PF.

The solid content was adjusted with methanol. Hence, deterioration of the mechanical properties of the resin with liginosulfonate-modified resins could partially be due to the solvent content. Kraft lignins are better suitable for dilution with organic solvents which is reflected by their better mechanical performance.

In a different study on mechanical properties of laminates conducted by Taverna et al. [56] the phenolic resins substituted with liginosulfonates resulted in better properties than with Kraft lignin: approximately 160 MPa in tensile strength, 220 MPa in flexural strength and 18 GPa in flexural modulus, versus 110 MPa in tensile strength, 200 MPa in flexural strength and 14 GPa in flexural modulus, respectively. In contrast to this previous investigation, in our present work, the substitution of

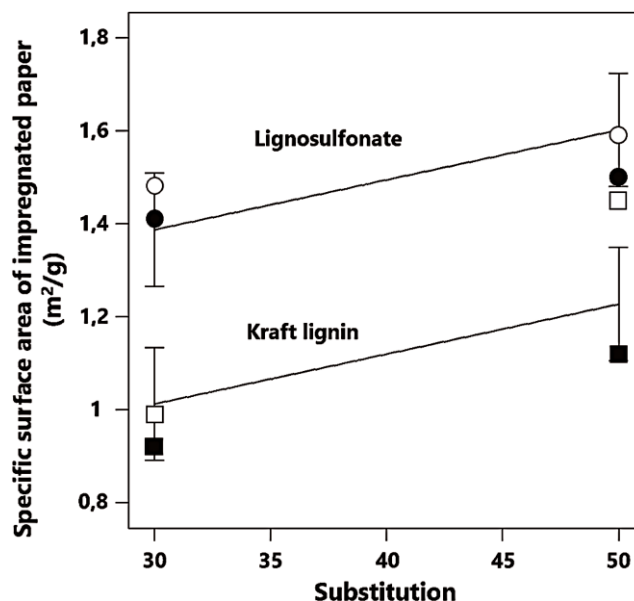


Figure 6: Effect of lignin type and degree of substitution on the pore volume of paper sheets impregnated with a variety of lignin-phenol hybrid resins. Circles (○, ●) represent lignosulfonate and squares (□, ■) represent Kraft lignin containing lignin-phenolic hybrid resins. Open symbols represent resins without and black symbols resins with phenolation modification. (The line is meant as a guide for the eye to illustrate the magnitude of the observed effects. No presumption of strict linearity is intended.)

phenol was only 10% w/w and the lignins were subjected to a hydroxymethylation modification step with formaldehyde before being reacted with phenol at pH 9 in the resin preparation. Due to hydroxymethylation, the lignin molecules might turn more reactive than the ones in the present study without phenolation modification. Moreover, the lower degree of substitution of phenol (10% w/w instead of 30% and 50%), might not disturb the polymeric PF network to such a large extent and hence result in better mechanical properties. Finally, the better results of the resin with lignosulfonates might also be a consequence of their different ash content and of the structurally larger lignosulfonates in comparison to the Kraft-type lignin [56].

There is a correlation between the mechanical properties and the specific surface area of the pre-pregs (Fig. 8). The larger the remaining free surface area is of the impregnated paper, the more the mechanical properties deteriorate. This highlights the importance of a homogeneous resin distribution in the paper after impregnation. It is advantageous, that the resin distributes equally and fills most of the pores.

Furthermore, the rupture characteristics in the bending tests looked different. Laminates prepared with lignin-based resins but without phenolation tended to break rather abruptly, whereas the laminates made with phenolation modified lignin tended to bend progressively, sometimes without break. Fig. 9 illustrates this for the broken laminate specimens made with L50PF and LP50PF. The phenolation treatment might have improved the plastic behavior of the phenolic resin by improving the integration of lignin molecules into the phenol-formaldehyde network.

Tabs. 5–7 show the analysis of variance of the three factors lignin type, lignin amount and modification type on the mechanical characteristics of the paper laminates. Tensile strength, flexural strength and flexural modulus were highly correlated and depend only on the type of lignin used for phenol substitution. Fig. 10 displays the effects of the varied resin factors on the mechanical laminate properties.

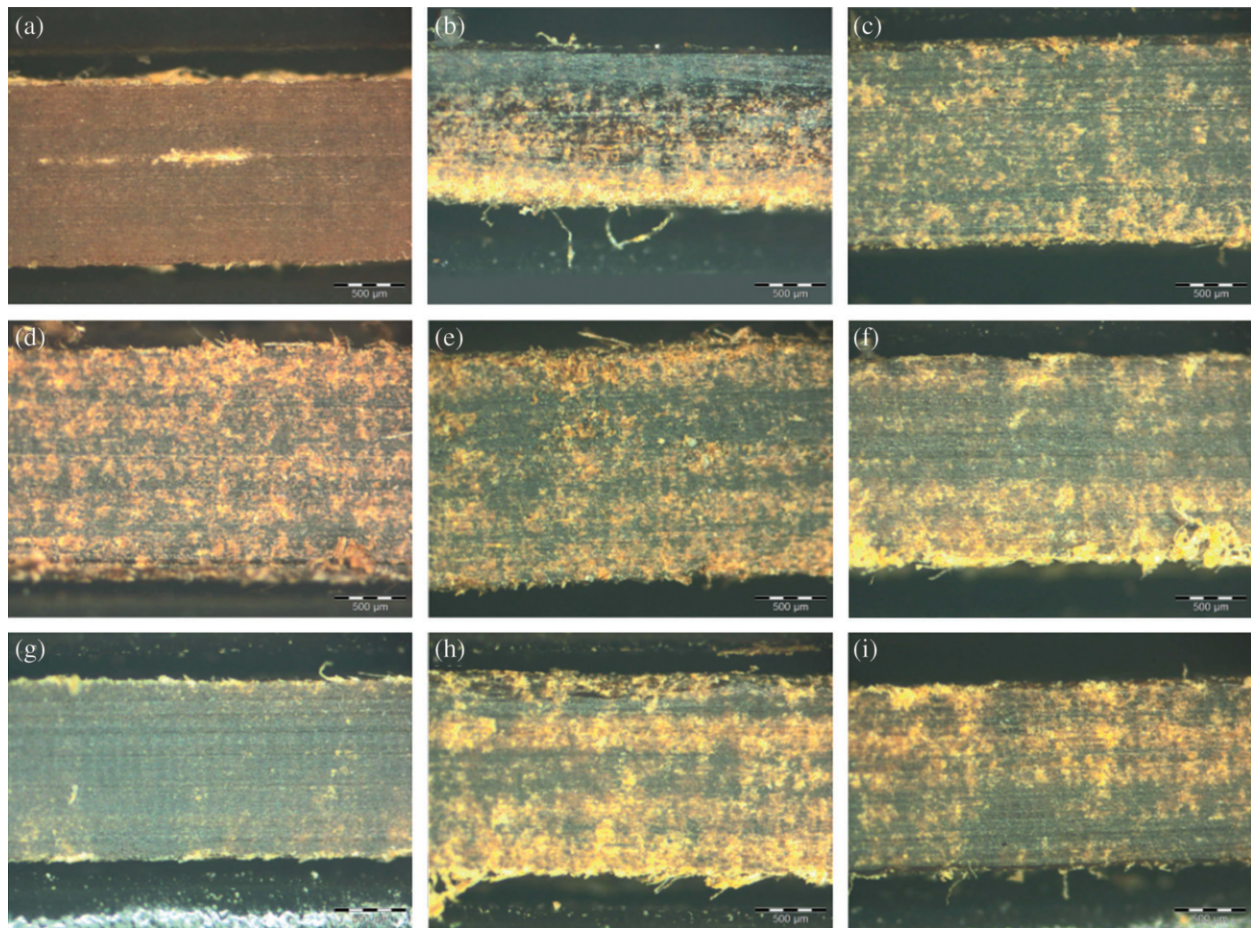


Figure 7: Photographs of cross sections of laminates made with the resins in methanol solvent (scale bar: 500 µm): (a) PF; (b) L30PF; (c) LP30PF; (d) L50PF; (e) LP50PF; (f) K30PF; (g) KP30PF; (h) K50PF; (i) KP50PF

Table 4: Density and mechanical characteristics of the 5-ply laminates made with the different resins

Resin	Density	Tensile strength (MPa)	Flexural strength (MPa)	Flexural modulus (GPa)
PF	1.38	133 ± 11.3	227.3 ± 31.9	17.5 ± 3.3
L30PF	1.29	67.3 ± 1.5	75.6 ± 0.2	5.3 ± 2.2
LP30PF	1.18	83.3 ± 7.4	145.2 ± 22.9	13.3 ± 3.5
L50PF	1.12	68.2 ± 5.7	121.4 ± 28.6	10.2 ± 2.8
LP50PF	1.08	63.2 ± 6.3	100.9 ± 33.7	8.5 ± 3.3
K30PF	1.30	111.5 ± 10.4	173.6 ± 34.5	14.9 ± 3.8
KP30PF	1.41	117.7 ± 8.1	202.5 ± 4.7	16 ± 0.9
K50PF	1.28	88.8 ± 10	158.8 ± 34.9	14.1 ± 3.3
KP50PF	1.28	127.5 ± 2.9	192.4 ± 20.5	15.6 ± 3.1

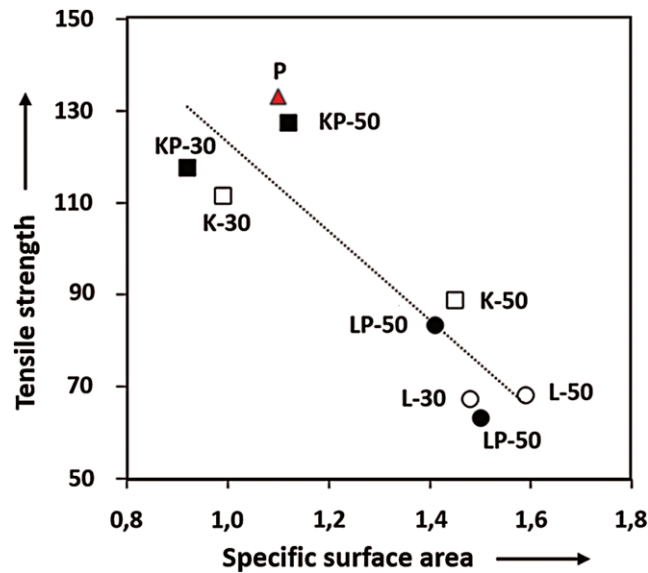


Figure 8: Correlation between specific surface area (“saturation”) of the impregnated paper and the mechanical performance (“tensile strength”)

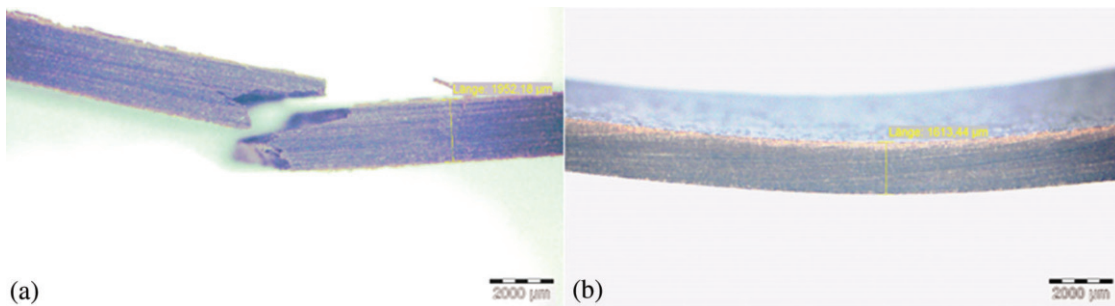


Figure 9: Laminates samples tested in mechanical flexural stress; (a) with L50PF (thickness: 1.95 mm); (b) with LP50PF (thickness: 1.61 mm)

Table 5: ANOVA analysis of the effects influencing the response “tensile strength“ of laminates prepared from the papers impregnated with the lignin-phenol hybrid resins

	Sum of Squares	F-value	p-value	R ²	R ² _{adjusted}	R ² _{predicted}
Model*	3341.53	19.24	0.0046	0.7622	0.7226	0.5773
Effects						
A: Lignin	3341.53	19.24	0.0046			−20.44
Residual	1042.33					

Table 6: ANOVA analysis of the effects influencing the response “flexural strength“ of laminates prepared from the papers impregnated with the lignin-phenol hybrid resins

	Sum of Squares	<i>F</i> -value	<i>p</i> -value	R^2	R^2_{adjusted}	$R^2_{\text{predicted}}$
Model*	10096.21	16.07	0.0070	0.7281	0.6828	0.5167
Effects						
A: Lignin	10096.21	16.07	0.0070			−35.53
Residual	3768.85					

Table 7: ANOVA analysis of the effects influencing the response “flexural modulus“ of laminates prepared from the papers impregnated with the lignin-phenol hybrid resins

	Sum of Squares	<i>F</i> -value	<i>p</i> -value	R^2	R^2_{adjusted}	$R^2_{\text{predicted}}$
Model*	67.86	11.46	0.0148	0.6553	0.5990	0.3890
Effects						
A: Lignin	67.86	11.46	0.0148			−2.91
Residual	35.54					

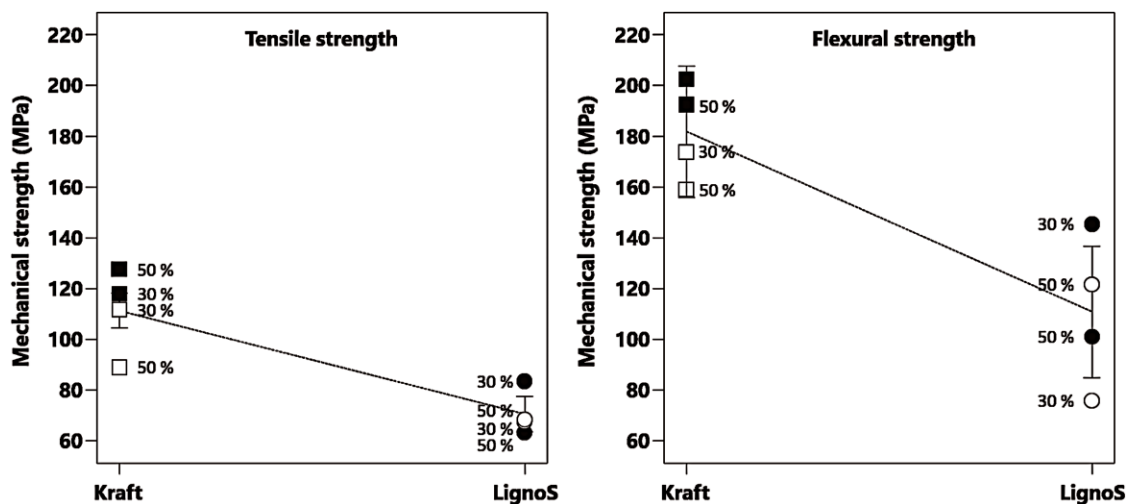


Figure 10: Effects of lignin type and amount on tensile and flexural strength of laminates. (The line is meant as a guide for the eye to illustrate the magnitude of the observed effects. No presumption of strict linearity is intended)

4 Conclusions

Phenolation treatment of the lignin before the resin synthesis with formaldehyde had a strong influence of the resin properties: the resins became less viscous when diluted, although their average molecular weight increased, their surface tension was generally higher, and the resulting laminates were mostly stronger in terms of mechanical properties. While it could be concluded prematurely that Kraft lignin hence is a better substituting material for phenol than are lignosulfonates; however, as highlighted in this present study, the properties relevant for impregnation do not only depend on the nature of lignin but also on the resin preparation procedure. Characterization of resin penetration into Kraft paper yielded interesting insights in the potential consequences of phenol substitution on the resulting laminates, after the impregnated papers were pressed and cured. Those resins that tended to deposit residues on the surface of the papers were identified as liquids with long penetration times (higher than 4 s). This leads to an inhomogeneous distribution of resin in the final laminate board, which resulted in minor mechanical properties.

Acknowledgement: The authors thank Dipl. Ing. Jörg Stultschnik for introducing the liquid-substrat penetration device and for performing some of the measurements on Kraft paper (grammage, mechanical properties, and Gurley air permeation). The authors further thank Dipl. Ing. Thomas Hardt-Stremayr who contributed to the mechanical tests of the laminates. Dr. Björn Geyer is greatly acknowledged for performing the IGC measurements on the paper samples.

Funding Statement: This work was carried out within the COMET program funded by the Austrian FFG, project number 844608.

Conflicts of Interest: The authors declared that they have no conflicts of interest.

References

1. Kandelbauer, A., Wuzella, G., Mahendran, A. R., Taudes, I., Widsten, P. (2009). Using isoconversional kinetic analysis of liquid melamine-formaldehyde resin curing to predict laminate surface properties. *Journal of Applied Polymer Science*, 113(4), 2649–2660. DOI 10.1002/app.30294.
2. Figueiredo, A. B., Evtuguin, D. V., Monteiro, J., Cardoso, E. F., Mena, P. C. et al. (2011). Structure–surface property relationships of kraft papers: implication on impregnation with phenol–formaldehyde resin. *Industrial & Engineering Chemistry Research*, 50(5), 2883–2890. DOI 10.1021/ie101912h.
3. Anonymus (2015). Phenolic Resins for Impregnation European Phenolic Resin Association. Accessed November 18, 2015. <http://www.epra.eu/21.html>.
4. Grenier-Loustalot, M. F., Larroque, S., Grande, D., Grenier, P., Bedel, D. (1996). Phenolic resins: 2. Influence of catalyst type on reaction mechanisms and kinetics. *Polymer*, 37(8), 1363–1369. DOI 10.1016/0032-3861(96)81133-5.
5. George, A., Sanjay, M. R., Srisuk, R., Parameswaranpillai, J., Siengchin, S. (2020). A comprehensive review on chemical properties and applications of biopolymers and their composites. *International Journal of Biological Macromolecules*, 154, 329–338. DOI 10.1016/j.ijbiomac.2020.03.120.
6. Zhu, Y., Romain, C., Williams, C. K. (2016). Sustainable polymers from renewable resources. *Nature*, 540(7633), 354–362. DOI 10.1038/nature21001.
7. Thomas, P., Duolikun, T., Rumjit, N. P., Moosavi, S., Lai, C. W. et al. (2020). Comprehensive review on nanocellulose: recent developments, challenges and future prospects. *Journal of the Mechanical Behavior of Biomedical Materials*, 110, 103884. DOI 10.1016/j.jmbbm.2020.103884.
8. Zhao, Z., Sun, S., Wu, D., Zhang, M., Huang, C. et al. (2019). Synthesis and characterization of sucrose and ammonium dihydrogen phosphate (SADP) adhesive for plywood. *Polymers*, 11(12), 1909.
9. Zhao, Z. Y., Hayashi, S., Xu, W., Wu, Z. H., Tanaka, S. et al. (2018). A novel eco-friendly wood adhesive composed by sucrose and ammonium dihydrogen phosphate. *Polymers*, 10(11), 1251. DOI 10.3390/polym10111251.

10. Zhao, Z., Sakai, S., Wu, D., Chen, Z., Zhu, N. et al. (2020). Investigation of synthesis mechanism, optimal hot-pressing conditions, and curing behavior of sucrose and ammonium dihydrogen phosphate adhesive. *Polymers*, *12(1)*, 216. DOI 10.3390/polym12010216.
11. Sun, S., Zhang, M., Umemura, K., Zhao, Z. (2019). Investigation and characterization of synthesis conditions on sucrose-ammonium dihydrogen phosphate (SADP) adhesive: bond performance and chemical transformation. *Materials*, *12(24)*, 4078. DOI 10.3390/ma12244078.
12. Kohlmayr, M., Zuckerstätter, G., Kandelbauer, A. (2011). Modification of melamine-formaldehyde resins by substances from renewable resources. *Journal of Applied Polymer Science*, *101(6)*, 4416–4423. DOI 10.1002/app.35438.
13. Umemura, K., Ueda, T., Kawai, S. (2012). Characterization of wood-based molding bonded with citric acid. *Journal of Wood Science*, *58(1)*, 38–45. DOI 10.1007/s10086-011-1214-x.
14. Zhao, Z., Sakai, S., Wu, D., Chen, Z., Zhu, N. et al. (2019). Further exploration of sucrose-citric acid adhesive: investigation of optimal hot-pressing conditions for plywood and curing behavior. *Polymers*, *11(12)*, 1996.
15. Sun, S., Zhao, Z., Umemura, K. (2019). Further exploration of sucrose-citric acid adhesive: synthesis and application on plywood. *Polymers*, *11(11)*, 1875. DOI 10.3390/polym11111875.
16. Jagadeesh, D., Kaanny, K., Prashanta, K. (2017). A review on research and development of green composites from plant protein-based polymers. *Polymer Composites*, *38(8)*, 1504–1518. DOI 10.1002/pc.23718.
17. Kang, H. J., Wang, Z., Wang, Y. Y., Zhao, S. J., Zhang, S. F. et al. (2019). Development of mainly plant protein-derived plywood bioadhesives via soy protein isolate fiber self-reinforced soybean meal composites. *Industrial Crops and Products*, *133*, 10–17. DOI 10.1016/j.indcrop.2019.03.022.
18. Li, F., Ye, Q. Q., Gao, Q., Chen, H., Shi, S. Q. et al. (2019). Facile fabrication of self-healable and antibacterial soy protein based films with high mechanical strength. *ACS Applied Materials & Interfaces*, *11(17)*, 16107–16116. DOI 10.1021/acsami.9b03725.
19. Wang, Z., Wen, Y. Y., Zhao, S. J., Zhang, W., Ji, Y. et al. (2019). Soy protein as a sustainable surfactant to functionalize boron nitride nanosheets and its application for preparing thermally conductive biobased composites. *Industrial Crops and Products*, *137*, 239–247. DOI 10.1016/j.indcrop.2019.04.054.
20. Uyama, H. (2018). Functional polymers from renewable plant oil. *Polymer Journal*, *50(11)*, 1003–1011. DOI 10.1038/s41428-018-0097-8.
21. Mucci, V. L., Hormaiztegui, M. E. V., Aranguren, M. I. (2020). Plant oil-based waterborne polyurethanes: a brief review. *Journal of Renewable Materials*, *8(6)*, 579–601. DOI 10.32604/jrm.2020.09455.
22. Mahendran, A. R., Aust, N., Wuzella, G., Kandelbauer, A. (2012). Synthesis and characterization of a bio-based resin from linseed oil. *Macromolecular Symposia*, *311(1)*, 18–27. DOI 10.1002/masy.201000134.
23. Mahendran, A. R., Wuzella, G., Aust, N., Kandelbauer, A., Müller, U. (2012). Photocrosslinkable modified vegetable oil based resin for wood surface coating application. *Progress in Organic Coatings*, *74(4)*, 697–704. DOI 10.1016/j.porgcoat.2011.09.027.
24. Wuzella, G., Mahendran, A. R., Müller, U., Kandelbauer, A., Teischinger, A. (2012). Photocrosslinking of an acrylated epoxidized linseed oil: kinetics and its application for optimized wood coatings. *Journal of Polymers and the Environment*, *20(4)*, 1063–1074. DOI 10.1007/s10924-012-0511-9.
25. Mahendran, A. R., Wuzella, G., Kandelbauer, A., Aust, N. (2012). Thermal cure kinetics of epoxidized linseed oil with anhydride hardener. *Journal of Thermal Analysis and Calorimetry*, *107(3)*, 989–998. DOI 10.1007/s10973-011-1585-7.
26. Mahendran, A. R., Aust, N., Wuzella, G., Müller, U., Kandelbauer, A. (2012). Bio-based non-isocyanate urethane derived from plant oil. *Journal of Polymers and the Environment*, *20(4)*, 926–931. DOI 10.1007/s10924-012-0491-9.
27. Hubbe, M., Pizzi, A., Zhang, A., Halis, H. R. et al. (2018). Critical links governing performance of self-binding and natural binders for hot-pressed reconstituted lignocellulosic board without added formaldehyde: a review. *Bioresources*, *13(1)*, 2049–2115. DOI 10.15376/biores.13.1.Hubbe.

28. Widsten, P., Hummer, A., Heathcote, C., Kandelbauer, A. (2009). A preliminary study of green production of fiberboard bonded with tannin and laccase in a wet process. *Holzforschung*, 63(5), 545–550. DOI 10.1515/HF.2009.090.
29. González-García, S., Feijoo, G., Heathcote, C., Kandelbauer, A., Moreira, M. et al. (2011). Environmental assessment of green hardboard production coupled with a laccase activated system. *Journal of Cleaner Production*, 19(5), 445–453. DOI 10.1016/j.jclepro.2010.10.016.
30. Wuzella, G., Mahendran, A., Bätge, R., Jury, T., Kandelbauer, A. S. (2011). Novel, binder-free fiber reinforced composites based on a renewable resource from the reed-like plant *Typha sp.* *Industrial Crops and Products*, 33(3), 683–689. DOI 10.1016/j.indcrop.2011.01.008.
31. Wuzella, G., Mahendran, A., Kandelbauer, R. A. (2020). Green composite material made from *Typha latifolia* fibres bonded with an epoxidized linseed oil/tall oil-based polyamide binder system. *Journal of Renewable Materials*, 8(5), 499–512. DOI 10.32604/jrm.2020.09615.
32. Shirmohammadli, Y., Efhamisizi, D., Pizzi, A. (2018). Tannins as a sustainable raw material for green chemistry: a review. *Industrial Crops and Products*, 126, 316–332. DOI 10.1016/j.indcrop.2018.10.034.
33. Ndiwe, B., Pizzi, A., Tibi, B., Danwe, R., Konai, N. et al. (2019). African tree bark exudate extracts as biohardeners of fully biosourced thermoset tannin adhesives for wood panels. *Industrial Crops and Products*, 132, 253–268. DOI 10.1016/j.indcrop.2019.02.023.
34. Xi, X., Pizzi, A., Frihart, C. R., Lorenz, L., Gerardin, C. (2020). Tannin plywood bioadhesives with non-volatile aldehydes generation by specific oxidation of mono and disaccharides. *International Journal of Adhesion and Adhesives*, 98, 102499. DOI 10.1016/j.ijadhadh.2019.102499.
35. Santiago-Medina, F. J., Basso, M. C., Pizzi, A., Delmotte, L. (2018). Polyurethanes from Kraft lignin without using isocyanates. *Journal of Renewable Materials*, 6(4), 413–425. DOI 10.7569/JRM.2017.634172.
36. Santiago-Medina, F. J., Pizzi, A., Basso, M. C., Delmotte, L., Abdalla, S. (2017). Polycondensation resins by lignin reaction with (Poly) amines. *Journal of Renewable Materials*, 5(5), 388–399. DOI 10.7569/JRM.2017.634142.
37. Younesi-Kordkheili, H., Pizzi, A. (2019). Some of physical and mechanical properties of particleboard panels bonded with phenol-lignin-glyoxal resin. *Journal of Adhesion*, 28, 1–11. DOI 10.1080/00218464.2019.1600405.
38. Younesi-Kordkheili, H., Pizzi, A. (2016). A comparison between lignin modified by ionic liquids and glyoxalated lignin as modifiers of urea-formaldehyde resin. *Journal of Adhesion*, 93(14), 1120–1130. DOI 10.1080/00218464.2016.1209741.
39. Younesi-Kordkheili, H., Pizzi, A., Niyatzade, G. (2015). Reduction of formaldehyde emission from particleboard by phenolated Kraft lignin. *Journal of Adhesion*, 92(6), 485–497. DOI 10.1080/00218464.2015.1046596.
40. Thébault, M., Müller, U., Kandelbauer, A., Zikulnig-Rusch, E., Lammer, H. (2017). Review on impregnation issues in laminates manufacture: opportunities and risks of phenol substitution by lignins or other natural phenols in resins. *European Journal of Wood and Wood Products*, 75(6), 853–876. DOI 10.1007/s00107-017-1206-7.
41. Vázquez, G., González, J., Freire, S., Antorrena, G. (1997). Effect of chemical modification of lignin on the gluebond performance of lignin-phenolic resins. *Bioresource Technology*, 60(3), 191–198. DOI 10.1016/S0960-8524(97)00030-8.
42. Ghorbani, M., Liebner, F., Van Herwijnen, H. W. G., Pfungen, L., Krahofer, M. et al. (2016). Lignin phenol formaldehyde resoles: the impact of lignin type on adhesive properties. *BioResources*, 11(3), 6727–6741. DOI 10.15376/biores.11.3.6727-6741.
43. Zhang, W., Ma, Y., Wang, C., Li, S., Zhang, M. et al. (2013). Preparation and properties of lignin-phenol-formaldehyde resins based on different biorefinery residues of agricultural biomass. *Industrial Crops and Products*, 43, 326–333. DOI 10.1016/j.indcrop.2012.07.037.
44. Ysbrandy, R. E., Sanderson, R. D., Gerischer, G. F. R. (1991). DSC thermal analysis of phenol and phenol-lignin extended resols and their physical behavior in paper laminates. *Papier*, 45, 62–67.
45. Ysbrandy, R. E., Sanderson, R. D., Gerischer, G. F. R. (1992). Adhesives from autohydrolysis bagasse lignin, a renewable resource. Part I. The physical properties of laminates made with phenolated lignin novolacs. *Holzforschung*, 46(3), 253–256. DOI 10.1515/hfsg.1992.46.3.253.

46. Mahendran, A. R., Wuzella, G., Kandelbauer, A. (2010). Thermal characterization of kraft lignin phenol-formaldehyde resin for paper impregnation. *Journal of Adhesion Science and Technology*, 24(8–10), 1553–1565. DOI 10.1163/016942410X500936.
47. Ghorbani, M., Mahendran, A. R., van Herwijnen, H. W. G., Liebner, F., Konnerth, J. (2017). Paper-based laminates produced with kraft lignin-rich phenol-formaldehyde resoles meet requirements for outdoor usage. *European Journal of Wood and Wood Products*, 76, 1–7.
48. Hubert, P., Poursartip, A. (2016). A review of flow and compaction modelling relevant to thermoset matrix laminate processing. *Journal of Reinforced Plastics and Composites*, 17(4), 286–318. DOI 10.1177/073168449801700402.
49. Roberts, R. J., Evans, P. D. (2005). Effects of manufacturing variables on surface quality and distribution of melamine formaldehyde resin in paper laminates. *Composites Part A: Applied Science and Manufacturing*, 36(1), 95–104. DOI 10.1016/S1359-835X(04)00127-7.
50. Thébault, M., Kutuzova, L., Jury, S., Eicher, I., Zikulnig-Rusch, E. M. et al. (2020). Effect of phenolation, Lignin-type and degree of substitution on the properties of lignin-modified phenol-formaldehyde impregnation resins: molecular weight, wetting behavior, rheological properties and thermal curing profiles. *Journal of Renewable Materials*, 8(6), 603–630. DOI 10.32604/jrm.2020.09616.
51. Thébault, M., Kandelbauer, A., Müller, U., Zikulnig-Rusch, E., Lammer, H. (2017). Factors influencing the processing and technological properties of laminates based on phenolic resin impregnated papers. *European Journal of Wood and Wood Products*, 75(5), 785–806. DOI 10.1007/s00107-017-1205-8.
52. Hochsteiner, S., Lenz, S., Stultschnik, J. (2016). Measuring device and measuring method for measuring the resin impregnation of a substrate. *Austrian Patent Application, Patent no. AT517076A4*.
53. Thébault, M., Kandelbauer, A., Zikulnig-Rusch, E., Putz, R., Jury, S. et al. (2018). Impact of phenolic resin preparation on its properties and its penetration behavior in Kraft paper. *European Polymer Journal*, 104, 90–98. DOI 10.1016/j.eurpolymj.2018.05.003.
54. Matsushita, Y., Wada, S., Fukushima, K., Yasuda, S. (2006). Surface characteristics of phenol-formaldehyde-lignin resin determined by contact angle measurement and inverse gas chromatography. *Industrial Crops and Products*, 23(2), 115–121. DOI 10.1016/j.indcrop.2005.04.004.
55. Thébault, M., Kandelbauer, A., Eicher, I., Geyer, B., Zikulnig-Rusch, E. (2018). Properties data of phenolic resins synthesized for the impregnation of saturating kraft paper. *Data in Brief*, 20, 345–352. DOI 10.1016/j.dib.2018.07.006.
56. Taverna, M. E., Ollearo, R., Morán, J., Nicolau, V., Estenoz, D. et al. (2015). Mechanical evaluation of laminates based on phenolic resins using lignins as partial substitutes for phenol. *BioResources*, 10(4), 8325–8338. DOI 10.15376/biores.10.4.8325-8338.